

The Carina spiral feature: Strömgren- β photometry approach

II. Distances and space distribution of the O and B stars[★]

N. Kaltcheva and M. Scorcio

Department of Physics & Astronomy, University of Wisconsin Oshkosh, 800 Algoma Blvd., Oshkosh, WI 54901-8644, USA
e-mail: kaltchev@uwosh.edu

Received 2 October 2009 / Accepted 29 January 2010

ABSTRACT

Aims. In recent years a significant development has become evident in the study of the stellar structure of the Galactic disk. This is especially true for the 3rd Galactic quadrant, where the stellar population was extensively investigated beyond 10 kpc, revealing details about the warped geometry of the thin and thick disks and outer arm. The 4th Galactic quadrant offers even better opportunity to follow the distribution of the young stellar populace to a large distance, since the line of sight is parallel to the largest single segment of a spiral arm seen from our position in the Galaxy: the Carina spiral feature. This paper further contributes to the study of the structure of the Galactic disk in the direction of Carina field utilizing homogeneous photometric distances of a sample of about 600 bright early-type stars seen in this direction up to 6 kpc.

Methods. The derived stellar distances are based on *uvby β* photometry. All O and B type stars with *uvby β* data presently available are included in the study.

Results. The photometry-derived parameters allow us to study the structure and characteristics of this segment of the Carina arm. We find that the stellar distribution is consistent with a location of the apparent edge of the arm at $l = 287^\circ$. Toward the edge of the arm the warp of the Galactic plane can be traced up to 6 kpc where it reaches negative 200 pc. The field toward the edge seems to be much more complex than harboring just one OB association, and it is likely that some of the apparent concentrations in this field represent parts of long segments of the edge. In the 284° – 289° longitude range an interarm space about 1 kpc wide is found beyond 850 pc from the Sun. The giant molecular clouds and open clusters do not follow the edge of the arm as defined by the OB stars and indicate a possible presence of an age gradient in a direction perpendicular to the formal Galactic plane.

Key words. Galaxy: structure – stars: distances – open clusters and associations: general

1. Introduction

The detailed structure of the Galactic spiral arms as delineated by the young stars and their groupings provides valuable information about the geometry of the thin and thick disk components. Tracing distant spiral features is, however, a complex experiment, heavily dependent on individual studies of the Galactic open clusters and OB-associations, and on the homogeneity and completeness of the available catalogs. Nevertheless, in recent years significant progress has been achieved in mapping the young stellar population within the disk to great distances. Examples include a topographical study of the Galactic disk from a sample of young open clusters to a distance of 4 kpc (Alfaro et al. 1991) and a study of the vertical profile of the Carina arm (Alfaro et al. 1992). Another detailed photometric investigation of the stellar population toward the CMa overdensity (Vázquez et al. 2008, and the reference therein) provides a comprehensive picture of the Local and outer spiral fragments in the third Galactic quadrant as well as of the warped geometry of the Galactic disk.

The focus of this article is the Carina section of the Milky Way, which is still considered to be the most promising of all fields for the optical study of a single large-scale Galactic feature (Bok 1937; Graham 1970). Observational efforts date back more

than a century to the pioneering work of Herschel & See on the apparent stellar clustering around η Car (See 1897). At one point Carina was even considered to be the center of our stellar system (Charlier 1916; Trumpler 1930). Becker (1956) and Bok (1956) originally suggested that this impressive apparent concentration of young stars is a tangentially observed segment of a spiral arm. Graham & Lynga's (1965) objective prism survey revealed that there are faint OB-stars as distant as 8–10 kpc. As early radio maps would show, this concentration is real, and not simply due to an absorption gap. However, the interstellar extinction toward Carina is low, allowing for observation of the structure to great distances. Probably the first comprehensive review of the Carina star-forming field was presented by Sher (1965), who compiled the results of the more than eighty major papers that existed at the time. The first mapping of the field was based on *UBV* photometry of a dozen open clusters (see Sher 1965). Later Bok et al. (1970) presented the first diagram of the structure of the field based both on clusters and field stars. Moffat & Vogt (1975) studied about 20 major clusters in Carina in terms of *UBV β* photometry. More recent photometric studies utilizing *uvby β* photometry were performed by Kaltcheva & Georgiev (1993), Shobbrook & Lynga (1994), Kaltcheva (1998), and Kaltcheva et al. (2000). A data-base collating all *uvby β* photometry available at present for O-B9 stars brighter than about 10th visual magnitude in the field of the Carina spiral feature is presented by Kaltcheva (2003, Paper I).

[★] Table 4 is only available in electronic form at the CDS via anonymous ftp to cdsarc.u-strasbg.fr (130.79.128.5) or via <http://cdsweb.u-strasbg.fr/cgi-bin/qcat?J/A+A/514/A59>

Table 1. Completeness of the sample across the field.

Range in Galactic longitude	No of stars with complete photometry	No of stars without complete photometry	Total number of stars	Completeness in %
282° to 284°	19	12	31	61
284° to 286°	86	79	165	52
286° to 288°	131	136	267	49
288° to 290°	99	107	206	48
290° to 292°	123	101	224	55
292° to 294°	44	79	123	36
294° to 296°	96	59	155	62

Here we provide precise *wbyβ* photometric distances for most of the stars with complete photometry included in Kaltcheva’s (2003) catalog and use them to outline the overall structure and characteristics of the Carina spiral feature. A detailed description of the photometric quantities used in this photometric system can be found in Strömberg (1966). Among the wide variety of photometric systems available today the *wbyβ* photometry is arguably better suited for the study of individual stars in terms of stellar luminosity than any other photometric system in wide use and proven to provide reliable stellar distances (cf. Kaltcheva & Makarov 2007). The derived distances and color excesses present a basis for establishing a homogeneous distance scale for the prominent stellar groupings in the Carina Field that will be carried out in the third paper of this series.

2. The sample

Our sample consists of about 600 stars earlier than A0 spectral type with available *wbyβ* photometry listed in at least one of the HD, CPD, PPM and LS catalogs. This excludes stars in clusters that do not have designations in the above catalogs, like for example most of the stars in Tr 16. The completeness of the sample over the apparent magnitude range is discussed in detail by Kaltcheva (2003). The limitations of the above catalogs set the magnitude limit for the sample at about 10th visual mag. Another restriction comes from the lack of spectral classification for the faint stars in the above catalogs. The overall completeness of the *wbyβ* database (Paper I) is quite satisfactory for stars brighter than 8.5 mag, dropping rapidly toward the fainter stars to less than 30% for the 9.5–10 visual magnitude range. However, the data-base is about 80% complete to 9.1 mag. The sample is magnitude-limited, which poses restrictions when studying the structure of star-forming fields. Nevertheless, the precise photometric distances derived here present a significant improvement over the current situation and should allow us to obtain reliable average distances for the apparent structures and substructures in the Carina field.

Table 1 shows the completeness of the sample as a function of Galactic longitude. The completeness is calculated in terms of number of stars from the above mentioned catalogs that have complete *wbyβ* photometry. The overall completeness is close to about 50%, with the 292°–294° range being an exception at a lower completeness of 36%.

Inspection of the reddening free $[c_1]/[m_1]$ diagrams (not included here) for the longitude ranges in Table 1 shows that half of the stars in the sample are earlier than B5. The spectral content of the sample is uniform over the longitude range.

3. Photometry-derived color excesses and distances

The procedure of deriving color excesses and stellar distances followed here is described in detail in Kaltcheva & Hilditch (2000) (KH hereafter). The color excesses were obtained via Crawford’s (1978) calibration for luminosity class (LC) V, IV and III and via the calibration by Kilkeny & Whittet (1985) for LC II, Ib, Iab and Ia. The sample used in this article does not contain stars with $[c_1] > 0.9$ mag, and thus no stars are expected to be found outside the limits of the intrinsic color calibrations. We used $R = 3.2$ and $E(B - V) = E(b - y)/0.74$ to obtain V_0 . The calibration of Balona & Shobbrook (1984) was utilized for all LC to derive the absolute magnitudes.

Since different calibrations are used to calculate the color excesses for different LC types, great care was taken to resolve all cases of suspected misclassification. To ensure a proper LC classification as possible, the database was divided into groups according to the LC available in Simbad and each group was considered separately. The reddening free $[c_1]/[m_1]$ and $[c_1]/\beta$ diagrams (not shown here) built for each LC were used to examine for possible LC misclassifications and for stars with H_β emission. It should be mentioned, however, that the presence of emission can complicate the photometric LC classification based on the $[c_1]/\beta$ diagrams. The individual sources of spectral classification were also considered for all cases of observed inconsistencies.

As is well known, the largest source of error in the calculated absolute magnitudes for early-type stars is the presence of emission lines in the stellar spectra. In general, within a given LC, a discrepancy between the observed β and the one calculated from the dereddened index c_0 ($\beta(c_0)$ hereafter), may indicate emission in the stellar spectrum, though sometimes the effect can be due to stellar evolution. As discussed in KH, for the brightest supergiants and all stars observed in emission, $\beta(c_0)$ should be used to calculate M_V . A comparison of the M_V values obtained with the calculated $\beta(c_0)$ ($M_V(c_0)$ hereafter) to the M_V values obtained via the observed β ($M_V(\beta)$ hereafter) can even better indicate stars observed in emission.

Our sample contains 130 stars classified as LC II-III, III. The photometric classification based both on $[c_1]/[m_1]$ and $[c_1]/\beta$ diagrams agrees with stars close to the main sequence. Seven of these stars are located above the LC II intrinsic color line in the $[c_1]/\beta$ diagram, exhibiting photometric behavior consistent with emission. For these stars $M_V(c_0)$ was adopted as a final estimate of the absolute magnitude.

The LC III-IV, IV, V group contains 197 stars. Of these 173 were assigned to the group because of their Simbad classification. Five stars have $\beta < 2.515$ and thus fell outside the limits of the Balona & Shobbrook (1984) calibration. For them $M_V(c_0)$ was used. Nine stars appear to be emission-line stars and $M_V(c_0)$ was adopted as a final estimate of the absolute magnitude for them as well. The remaining 24 stars of this group are classified in the Simbad database as LC II, but showed a systematic disagreement between their $M_V(c_0)$ and $M_V(\beta)$ values when treated as LC II. A close examination of the dereddened $[c_1]$ vs. β diagram pointed to a possible LC misclassification. Based on their photometric behavior, we adopted a LC III for these stars and recalculated the color excess with Crawford’s (1978) calibration, which removed the systematic difference. These stars are listed in Table 2.

In the sample are 97 stars without available LC. Inspection of the photometric diagrams allowed those stars to be classified

Table 2. Stars originally classified as LC II in the Simbad data-base for which LC III was adopted.

HD 87752	HD 88623	HD 89683	HD 91525	HD 91198
HD 92143	HD 92237	HD 93071	HD 93621	HD 94987
HD 95018	HD 95085	HD 95121	HD 95172	HD 95863
HD 96523	HD 98227	HD 98584	HD 99500	HD 100465
HD 101330	HD 102010	HD 102237	HD 102248	

Table 3. Stars for which the β index calculated from c_0 is used to obtain M_V .

Ia
HD 91619V, HD 92850, HD 92964, HD 94304 HD 94367, HD 94369, HD 94909A, HD 96919V
Iab-Ib, Ib
HD 91969, HD 99953, HD 100943
Ib-II
HD 92420, HD 95880AB, HD 98410
III
HD 90599, HD 91188, HD 91943, HD 93563, HD 96864, HD 100199, HD 306791V
IV
HD 87471, HD 91598
V
HD 88825, HD 91269, HD 91465V, HD 92027, HD 93618 HD 93683 HD 96357, HD 97151, HD 98927, HD 99025 HD 99771, HD 305296
LC not available
CPD-60 3122, HD 90177V, HD 90187, HD 93561, HD 93632 HD 94910V, HD 96261B, HD 96264B, HD 97726V, HD 101794 HD 303075V, HD 303188, HD 303492, HD 305632, HD 305897 HD 306797V, HD 307350, HD 309467

as LC III-V. Among them there are 10 stars with $\beta < 2.515$ mag and eight emission-line stars. In both cases $M_V(c_0)$ was adopted.

For stars of LC I and II the $[c_1]/[m_1]$ diagram is not informative in terms of luminosity classification, thus only the $[c_1]/\beta$ diagrams were used to identify possible mis-classifications. The sample contains eight stars classified as Ia, Iae in the Simbad database, and that classification seems consistent with the photometric $[c_1]/\beta$ diagram. Following KH, $M_V(c_0)$ is adopted as a final estimate of the absolute magnitude for all Ia stars since β is expected to be influenced by emission for this LC. This procedure helped to obtain reasonable estimates of the absolute magnitude for four stars with very negative $M_V(\beta)$. The rest of the Ia stars showed good agreement between the $M_V(\beta)$ and $M_V(c_0)$ values. Luminosity class Iab was represented by six stars, most of which (especially HD 89714 and HD 95733) could be classified photometrically as Ib or even LC II based on the $[c_1]/\beta$ diagram. Keeping this in mind we used $M_V(\beta)$ for our final estimate of the absolute magnitude of all six Iab stars. In general there is a good agreement between $M_V(\beta)$ and $M_V(c_0)$ for all Iab stars, with the exception of HD 96248 (-8.1 mag vs. -5.1 mag). Luminosity class Ib contains 26 stars, of which $M_V(c_0)$ was adopted for only three stars. $M_V(c_0)$ was used among the 46 stars of LC Ib-II and II for another three stars instead of $M_V(\beta)$. All stars, for which a β index calculated from c_0 was used to obtain M_V , are listed in Table 3. Table 4, available only electronically

via CDS, summarizes the photometry-derived information for all 598 stars in the sample. The table contains star identification, spectral classification found in the Simbad data-base, the photometric quantities and the dereddened photometry and color excess, absolute magnitudes and the calculated distances. The stars are organized in groups according to their luminosity classes. The expected uncertainties in M_V are on the order of ± 0.3 for LC III-V and ± 0.5 for supergiants (Balona & Shobbrook 1984), which propagate to an asymmetric uncertainty of -13% to $+15\%$ and -21% to $+26\%$ in the derived distances, respectively.

4. Discussion

4.1. Comparisons to other surveys

It is worthwhile to compare our distance estimates to previous estimates available in the literature. Photometric distances of two large samples of early-type stars in Carina are published by Graham (1970) and Shobbrook & Lynga (1994). Graham (1970) used an $M_V(\beta)$ calibration obtained as an average of the calibrations of Fernie (1965) and Graham (1967), and broad-band photometric estimations of reddening to derive the distances. Shobbrook & Lynga (1994) applied the calibration of Balona & Shobbrook (1984), but the procedure utilized by these authors is slightly different from ours, mainly when applied to emission-line stars. Histograms of the differences in stellar distance in terms of “this paper minus others” are presented in Fig. 1. There are 98 stars in common between our survey and that of Graham (1970). If we omit seven stars with considerable differences, the average is -185 ± 850 pc (the uncertainties used throughout the text are the standard deviations, unless a different uncertainty is mentioned). The 43 stars in common with Shobbrook & Lynga (1994) have an average of the differences of -205 ± 450 pc (LS 1962 and LS 2089 are omitted). On average, the distances obtained here are smaller by 200 pc in comparison to the previous studies. Since our procedure of using $M_V(c_0)$ values for the emission line stars should eliminate distance overestimations, this is likely the cause of the discrepancy. The calculated standard deviations point to a better agreement between our results and that of Shobbrook & Lynga (1994) due to the use of the same calibration. The bottom plot in Fig. 1 presents the structure of the field as revealed by the stars in common with these authors. One can notice the similar distribution of the two sets with Galactic longitude. There are 40 stars in the Shobbrook & Lynga (1994) survey fainter than the limiting magnitude of our survey, and thus not included in our sample. With the relatively good agreement in the derived distances in mind, we include these stars in the following discussion using the distances calculated by Shobbrook & Lynga (1994).

4.2. Distribution of the stars in Galactic longitude

Figure 2 is a plot of the derived distance for each star as a function of Galactic longitude. Each LC discussed above is plotted separately. For LC II-III to V (first three diagrams) the stars with $M_V(c_0)$ adopted as a final estimate of the absolute magnitude are shown with filled symbols. It can be seen that these stars do not show any systematic trend in terms of distance in comparison to the rest of the sub-samples. Luminosity class III-IV, IV, V form a main layer of 124 stars between 270 and 1400 pc at a median distance of 754 ± 320 pc. The stars of LC II-III, III are spread out up to 2.5–3 kpc, while the “unclassified” stars (fainter in general) are mostly located beyond 2 kpc. The 40 stars taken from Shobbrook & Lynga (1994) are plotted together with the

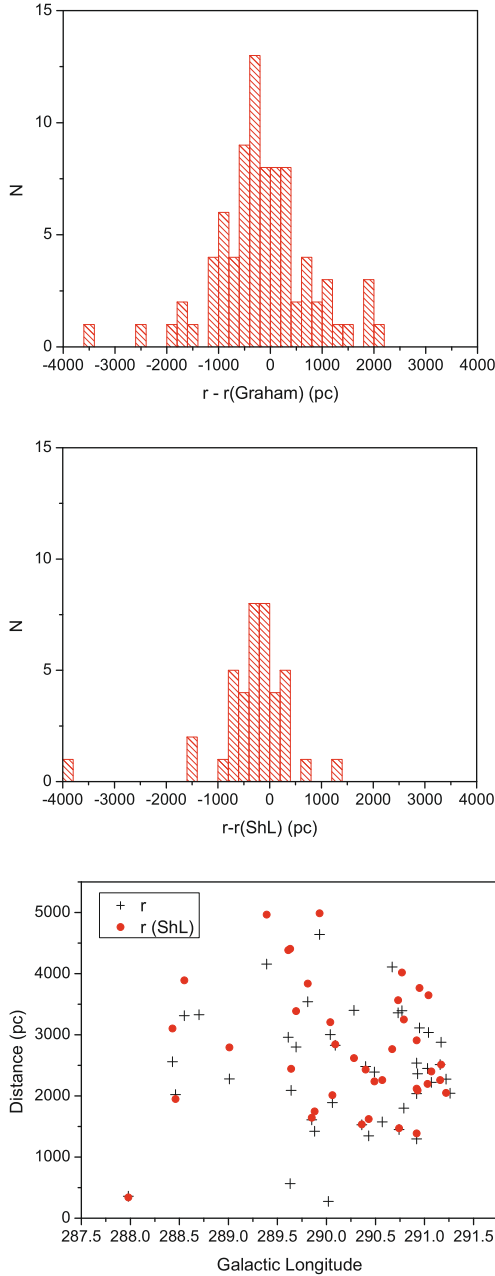


Fig. 1. The histograms of the differences between the photometric distances obtained here and those by Graham (1970) (*top panel*) and Shobbrook & Lynga (1994) (*middle panel*). The *bottom panel* presents a comparison of the location of the stars plotted as a function of Galactic longitude using the distances obtained here (plus symbols) and those calculated by Shobbrook & Lynga (1994) (filled symbols). The overall uncertainty in the plotted stellar distances is about 15%.

“unclassified” stars and fit well in the overall picture delineated by them. The LC I–II (fourth plot in Fig. 2) are located beyond 1 kpc in the 288°–292° longitude range and beyond 1.6 kpc toward 284°–287°.

Figure 3 presents all sample stars plotted in Galactic coordinates, the plots of photometric distances vs. Galactic longitude and Galactic latitude, and the color excess vs. Galactic longitude. The solid line on distances vs. Galactic longitude diagram is the apparent edge of the Carina arm as derived by Graham (1970). Figure 3 supports the conclusion of Graham (1970) that no early-type stars are found at great distances (greater than 4 kpc for our sample) for longitudes smaller than 286°.

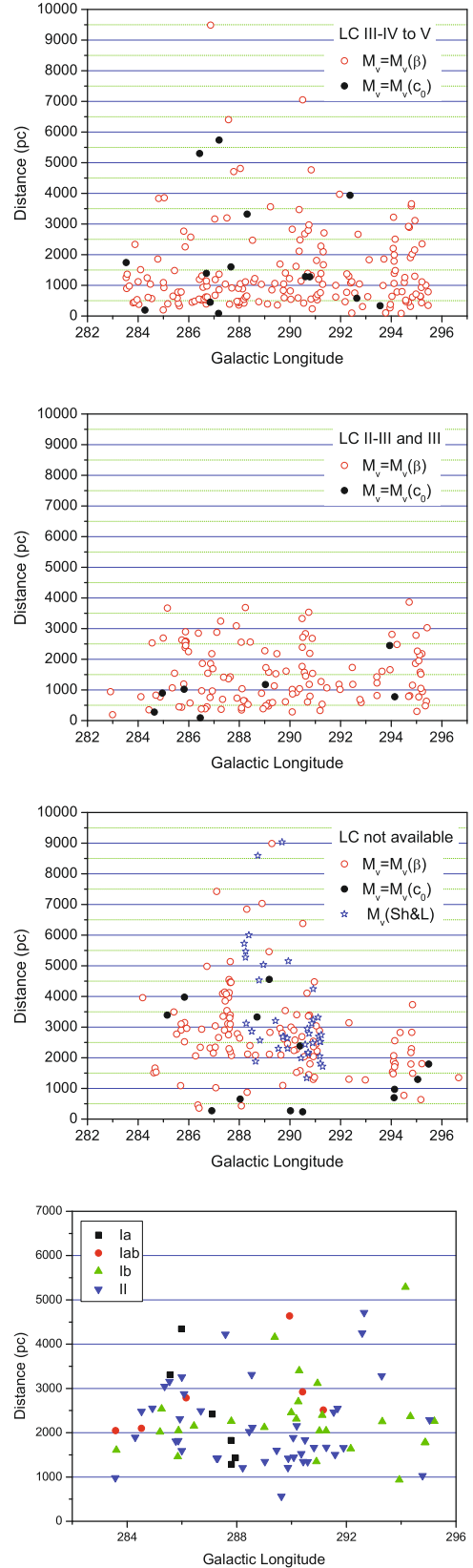


Fig. 2. Photometric distances plotted as a function of Galactic longitude for different LC groups. In the first three plots filled dark symbols are used for stars with $M_V(c_0)$ adopted as final estimate of the absolute magnitude. The 40 stars taken from Shobbrook & Lynga (1994) are included in the third plot as open-star symbols. In the first three plots, the overall uncertainties in the used distances are about 15%. In the last diagram, the stars of LC Ia, Ia b, Ib and II are plotted with different symbols as indicated on the panel, and the overall uncertainty is about 23%.

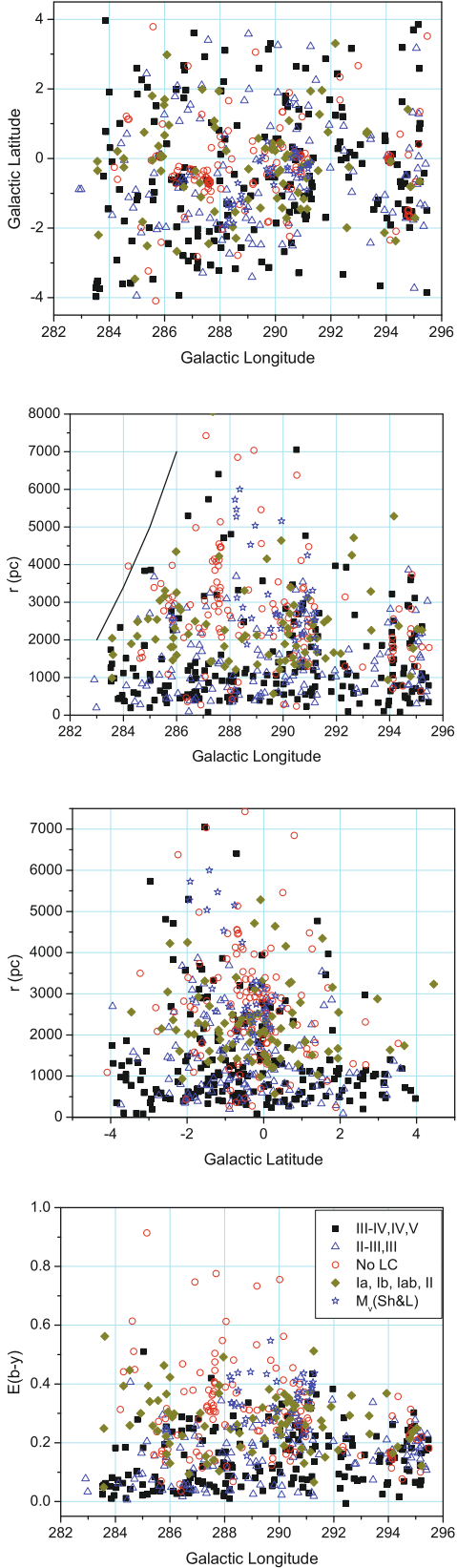


Fig. 3. Sample stars plotted in Galactic coordinates and the photometric distances and color excesses plotted as a function of the Galactic coordinates. The stars are marked with different symbols according to their LC as follows: filled squares – LC III-IV, IV, V; open triangles – LC II-III, III; open circles – the group without LC available, filled diamonds – LC Ia, Ib, Iab, II. The 40 stars from Shobbrook & Lynga (1994) are shown with open-star symbols on all diagrams. The uncertainties in the stellar distances are the same as in Fig. 2.

outer edge of the Carina arm, as proposed by the same author, seems consistent with the structure revealed by the present sample. For our sample, however, very few stars are seen at large distances for longitudes greater than 291° as well, where the completeness is less than 50%. Since for distances greater than 3–4 kpc, the observational selection effects are severe, a much broader and fainter sample is needed for reliable conclusions. In the 284° – 289° longitude range there is an indication of an inter-arm space between 1 and 2 kpc that separates the relatively nearby structure consisting mainly of III-V LC stars from the structure of slightly more-luminous stars located beyond 2 kpc. The presence of an inter-arm space is also supported by the gap in the color excess seen in the fourth plot in Fig. 3. A similar feature was noticed by Kaltcheva (1998) based on a much smaller sample. Contrarily to that, toward $l = 291^\circ$ most of the stars are spread out in depth between 1 and 3 kpc. This is the line of sight toward the Car OB2 association. The new larger sample confirms the previous conclusions (Shobbrook & Lynga 1994; Kaltcheva 1998) of a grouping in this direction spread out in depth over a range larger than 1 kpc.

4.3. Distribution perpendicular to the Galactic plane

It was already demonstrated by a number of authors that spiral arm tracers tend to lie below the Galactic plane for great distances in the Carina direction (Graham 1970; Shobbrook & Lynga 1994 and the references therein). Probably the most comprehensive investigation of the Galactic warp in the southern sky that includes the Carina section was presented by Reed (1996). His study, based on a sample of 1300 OB stars with available $UBV\beta$ photometry, found evidence of a warp reaching -1.5 kpc at a galacto-centric distance of 15 kpc and $l = 280^\circ$.

The plot of distance vs. Galactic latitude in Fig. 3 indicates that the majority of the stars in the sample more distant than 2 kpc are located between 0.5° and -2° Galactic latitude. Figure 4 presents the distance Z from the Galactic plane plotted against the distance r from the Sun for three longitudinal intervals: 283° – 288.6° , 288.6° – 291.6° and 291.6° – 296° , with the aim to study the distribution of the stars perpendicular to the Galactic plane at different longitudes. According to Graham (1970) the outer edge of the Carina arm is parallel to the direction 287° , which falls in the first longitudinal interval. The second interval contains the large apparent concentration toward Car OB2. The solid line on each Z vs. r diagram is the relation obtained by Graham (1970) for the average location of the OB-stars toward Carina. The diagrams on the right side of Fig. 4 present the stellar content in each of the three longitudinal intervals. In Fig. 4 the following symbols are used: plus symbols for stars of LC V-III with $M_V - 3$ mag and brighter, filled symbols for stars of LC V-III with $M_V > -3$ mag, open symbols for stars of LC I-II that are still close to the main sequence and filled triangles for evolved stars of LC I-II. The 40 stars from Shobbrook & Lynga (1994) are shown with open-star symbols on the Z vs. r diagrams.

As expected, in all three longitudinal intervals the stars less luminous than -3 mag are found closer than 2 kpc in general, due to the effect of the limiting magnitude of the survey. In the first Galactic longitude range (284° – 288.6°), the majority of the intrinsically bright stars ($M_V < -3$) closely follow the relation proposed by Graham (1970). Our sample allows us to trace the outer edge of the Carina arm up to 6 kpc. At a distance of 6 kpc, the stars in the sample show a warp of about negative 200 pc, a value similar to the one that can be obtained from the plots presented by Reed (1996).

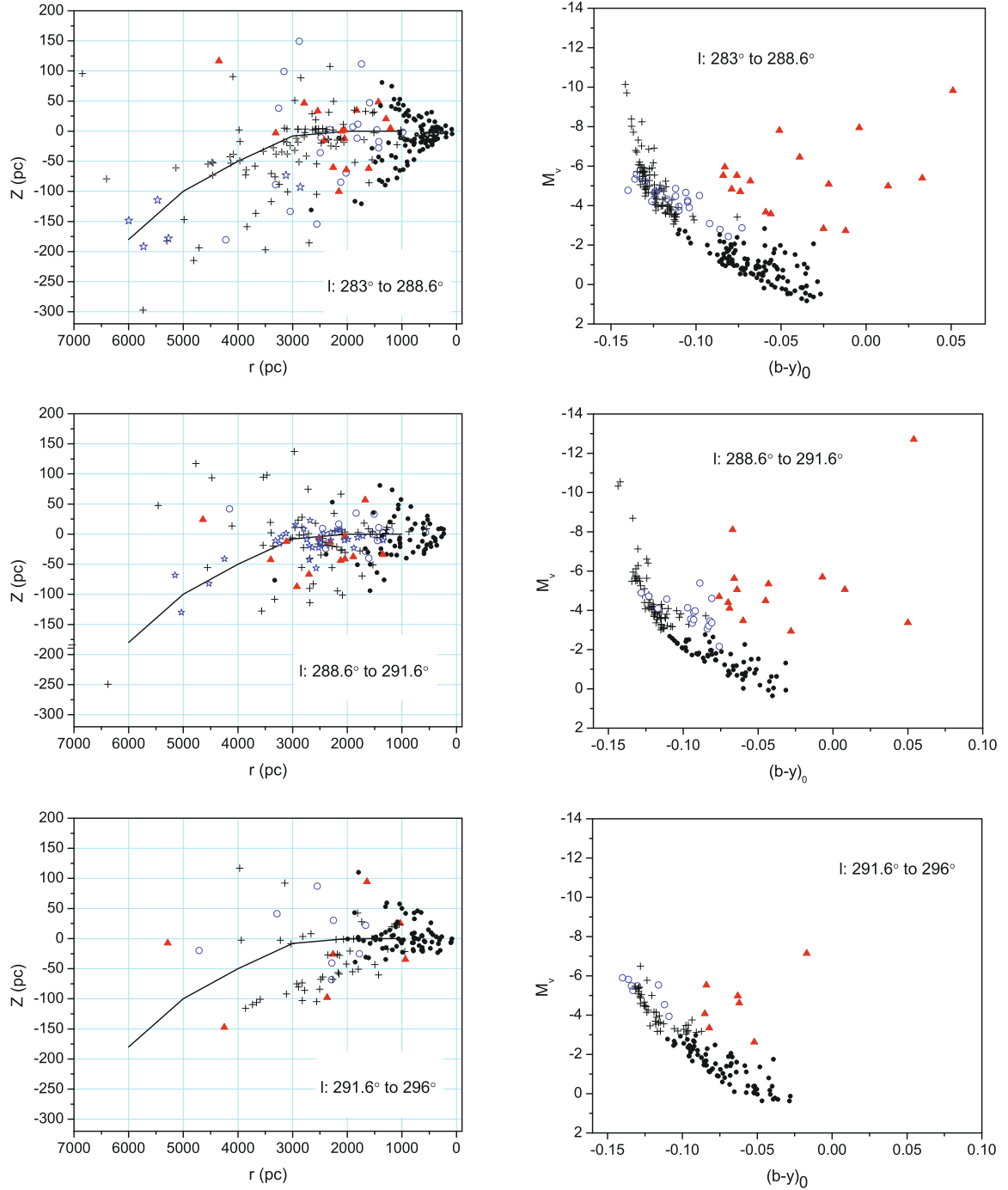


Fig. 4. Distance Z from the Galactic plane plotted against distance from the Sun for three longitude intervals. The solid line is the relation obtained by Graham (1970). The following symbols are used: plus symbols for stars of LC V-III with $M_V - 3$ mag and brighter; filled symbols for stars of LC V-III, with $M_V > -3$ mag, open symbols for stars of LC I to II that are still close to the main sequence; and filled triangles for evolved stars of LC I to II. The 40 stars from Shobbrook & Lynga (1994) are shown with open-star symbols on the Z vs. r diagrams. The uncertainties in the stellar distances are the same as in Fig. 2.

An interesting feature of the M_V vs. $(b - y)_0$ diagram for this longitude range is the presence of very few stars in the -2 to -3 range in M_V . In the Z vs. r plot, there is a clear spatial separation of about 900 – 1000 pc between the intrinsically bright stars (plus symbols) and the fainter stars (filled symbols). This feature is also seen in the r vs. l plot (Fig. 3) and points out that an inter-arm-like space exists between the nearby young structures and the edge of the Carina arm within the formal Galactic plane. The stars of LC I-II are quite spread out with no obvious concentration along the edge. In the second longitude interval the sample

still follows the Graham's line and the warp can be traced up to 5 kpc. No inter-arm space is obvious. There is a tendency of the evolved stars of LC I-II to be located at and below the plane. In the third longitude interval most of the intrinsically bright stars are located below or above the plane and the sample does not follow the Graham's line. Note that toward $l = 292^\circ$ the sample is quite incomplete and consists of mostly nearby stars. The stars located below the formal plane are all found at longitudes larger than 293° and indicate that the bending below the plane begins at 1.5 kpc at this longitude.

4.4. The field between 284° – 288.6° Galactic longitude

This longitudinal interval contains the outer edge of the Carina arm parallel to the direction 287° . The edge of the arm is best defined by the stars of LC V-III intrinsically brighter than -3 mag (marked with plus symbols in Fig. 4). Figure 5 presents these stars in the 284° – 288.6° longitude interval plotted in Galactic coordinates (a), the distance Z from the plane plotted vs. distance from the Sun (b), and the photometric V_0 vs. $(b-y)_0$ and M_V vs. $(b-y)_0$ diagrams (c, d). Open symbols are used for these of them that do not follow closely the Graham’s line. According to Humphreys (1978) this region is dominated by the Car OB1 association ($284.2^\circ < l < 288^\circ$, $-2.2^\circ < b < 0.9^\circ$) at 2.5 kpc. In their revision of the list of Galactic OB associations Mel’nik & Efremov (1995) break down Car OB1 into five groups at distances between 2.2 and 2.8 kpc.

In Fig. 5 different symbols are used to denote the apparent groups that could be separated toward the edge based on the sample used in this subsection. The group marked with plus-symbols (23 stars) is located at the average coordinates $l = 287.56^\circ$, $b = -0.67^\circ$. These coordinates are very similar to those of the Car 1E group ($l = 287.61^\circ$, $b = -0.68^\circ$, at 2.64 kpc) from the list of Mel’nik & Efremov (1995). This falls in the direction toward η Car as well. According to the distances obtained here, these stars are spread out between 2204 and 6404 pc, with an average of 3728 ± 956 pc. Another apparent concentration is marked with filled squares (six stars) at $l = 287.01^\circ$ and $b = -0.41^\circ$ and average distance of 3308 ± 2090 pc. The significant spread in distance suggests that these are not physical groups. The third apparent grouping, marked with open triangles (16 stars) is found at $l = 285.83^\circ$ and $b = 0.071^\circ$. The location of this group is similar to that of Car 1B at $l = 285.98^\circ$, $b = 0.40^\circ$ from the list of Mel’nik & Efremov (1995). These stars are well grouped according to their individual distances, and the density profile reveals one group at a median distance of 2583 ± 70 (s.e.) pc.

Apparently this region is much more complex than harboring just one stellar association. It seems that it contains projections of stars located along the outer edge of the Carina arm. The spread of these stars along the line of sight is much more extended than the expected spread due to errors in distance determination. Ninety percent of these stars are O-type. It is highly likely that some of these apparent concentrations represent parts of long segments of the outer edge of the Carina arm.

4.5. Distribution of open clusters and giant molecular clouds toward Carina

With the aim of tracing the outer edge of the Carina arm using different spiral structure indicators, the location of open clusters and giant molecular clouds (GMC) are plotted in Fig. 6. The data for the open clusters were extracted from the catalog of Dias et al. (2003). The clusters are marked with different symbols according to their age, as indicated on the panel. The data for the GMC were selected from the work of Grabelsky et al. (1988). The plots provide an impression about the Galactic stellar and molecular warp toward the outer edge of the Carina arm. Almost all of the clusters younger than 6.8 Myr are closely associated with GMC. Interestingly, the young clusters are all closely confined to the formal plane ($b = 0^\circ$), while the clusters older than 7.6 Myr are found well below the plane for distances greater than 1 kpc. This separation is best seen for the field between 283° and 291° longitude and might indicate a presence of age gradient in a direction perpendicular to the Galactic plane for this longitude

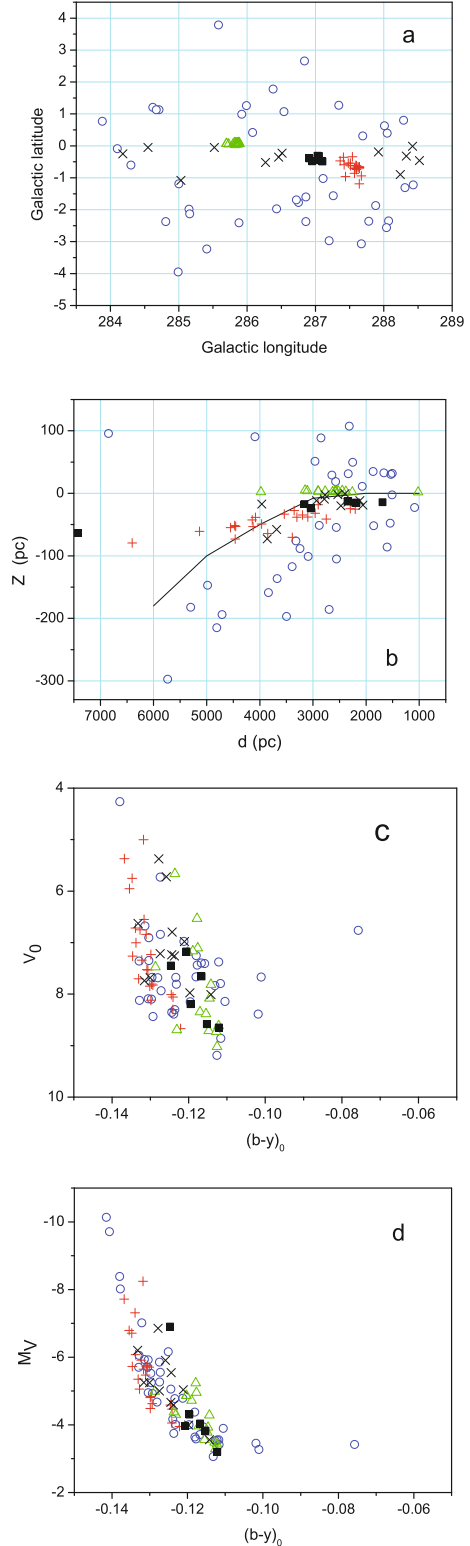


Fig. 5. Intrinsically bright ($M_V < -3$ mag) stars of LC V to II in the field between $l = 284^\circ$ and $l = 288.6^\circ$. **a)** The stars plotted in Galactic coordinates with different symbols to mark different apparent groups and layers. **b)** The distance Z from the Galactic plane plotted against the distance from Sun. **(c, d)** The V_0 vs. $(b-y)_0$ and M_V vs. $(b-y)_0$ diagrams. The overall uncertainties in the plotted distances are about 15%.

interval. The GMCs do not follow the outer edge as delineated by Graham (1970), and the bending below the plane is much less for these tracers than for the OB stars. The clusters also do not convincingly follow the edge.

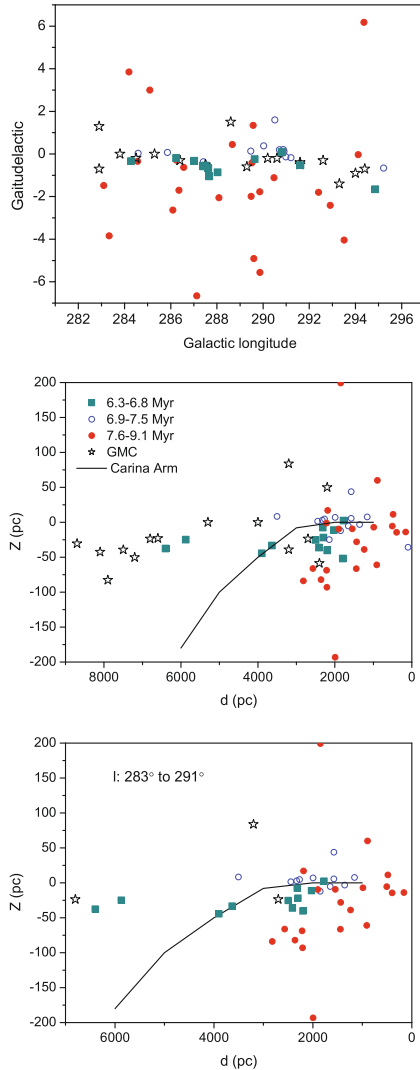


Fig. 6. Open clusters and giant molecular clouds in the field studied plotted in Galactic coordinates, and distance Z from the Galactic plane plotted against distance from Sun. Different symbols are used to mark clusters of different age, as indicated on the middle panel. The giant molecular clouds identified in the field are shown with open-star symbols. The solid line is the relation obtained by Graham (1970).

5. Conclusion

Precise homogeneous $uvby\beta$ stellar distances and reddening were derived for a sample of 598 O-B9-type stars in the field of the Carina spiral feature. Photometry-derived parameters allowed us to study the structure and characteristics of this segment of the Carina arm up to a distance of 6 kpc. The main findings of this investigation are:

1. The distribution of the stars in this sample is consistent with the location of the apparent edge of the Carina arm as derived by Graham (1970).
2. In the 284° – 289° longitude range an interarm space about 1 kpc wide was found beyond 850 pc from the Sun.
3. Toward $l = 291^{\circ}$ (this is the direction of Car OB2) the young stars are spread out in depth over a range larger than 1 kpc, and the interarm space is no longer evident.

4. Toward the edge of the arm ($l = 287^{\circ}$) the warp of the Galactic plane could be traced up to 6 kpc, where it reaches negative 200 pc. Toward $l = 294^{\circ}$ the sample stars do not delineate the edge of the arm any more and the bending below the plane begins at about 1500 pc from the Sun.
5. The field toward the edge of the Carina arm (this is the direction toward η Car) seems to be much more complex than harboring just one OB association. It is likely that some of the apparent concentrations in this field represent parts of long segments of the edge of the Carina arm.
6. The distribution of the GMC and known open clusters in the field does not follow the edge of the arm as defined by the OB stars. The oldest open clusters are predominantly located below the formal plane, indicating a possible age gradient perpendicular to the formal Galactic plane.

Acknowledgements. Support for this research was provided by the National Science Foundation grant AST-0708950. N.K. acknowledges support from the SNC Endowed Professorship and the University of Wisconsin Oshkosh sabbatical program. The authors deeply thank Dr. B. Cameron Reed for helpful discussions. We are grateful to the referee Dr. Willem Jan de Wit for a number of valuable comments. This research has made use of the SIMBAD database, operated at CDS, Strasbourg, France.

References

- Alfaro, E. J., Cabrera-Cano, J., & Delgado, A. J. 1991, The formation and evolution of star clusters (A93-48676 20-90), 133
- Alfaro, E. J., Cabrera-Cano, J., & Delgado, A. J. 1992, *ApJ*, 399, 576
- Balona, L. A. 1994, *MNRAS*, 267, 1060
- Balona, L. A., & Shobbrook, R. R. 1984, *MNRAS*, 211, 375
- Becker, W. 1956, *Vistas Astron.*, 2, 1515
- Bok, B. J. 1937, The distribution of the stars in space (Chicago: Univ. of Chicago Press)
- Bok, J. B. 1956, *Vistas Astron.*, 2, 1522
- Bok, J. B., Hine, A. A., & Miller, E. W. 1970, *Symp.*, 38 (Reidel: Dordrecht), 246
- Charlier, C. V. L. 1916, *Lund Medd.*, Ser. 2, 31
- Crawford, D. L. 1978, *AJ*, 83, 48
- Dias, W. S., Alessi, B. S., Moitinho, A., & Lépine, J. R. D. 2003, *EAS Publ. Ser.*, 10, 195
- Fernie, J. D. 1965, *AJ*, 70, 575
- Grabelsky, D. A., Cohen, R. S., Bronfman, L., & Thaddeus, P. 1988, *ApJ*, 331, 181
- Graham, J. A. 1967, *MNRAS*, 135, 377
- Graham, J. A. 1970, *AJ*, 75, 703
- Graham, J. A., & Lynga, G. 1965, *Memoirs of the Mount Stromlo Observatory*, Canberra: Austr. National University
- Humphreys, R. M. 1978, *AJSS*, 38, 309
- Kaltcheva, N. 2003, *A&A*, 410, 523
- Kaltcheva, N., & Hilditch, R. 2000, *MNRAS*, 312, 753
- Kaltcheva, N., & Makarov, V. 2007, *ApJ*, 667, L155
- Kaltcheva, N. T. 1998, *A&AS*, 128, 309
- Kaltcheva, N. T., & Georgiev, L. N. 1993, *MNRAS*, 261, 846
- Kaltcheva, N. T., Olsen, E. H., & Clausen, J. V. 2000, *A&AS*, 146, 365
- Kilkenny, D., & Whittet, D. C. B. 1985, *MNRAS*, 216, 127
- Mel'nik, A. M., & Efremov, Yu. N. 1995, *Astron. Lett.*, 21, 13
- Moffat, A. F. J., & Vogt, N. 1975, *A&AS*, 20, 125
- Ruprecht, J., Balazs, B., & White, R. E. 1981, *Catalogue of Star Clusters and Associations*, ed. B. Balazs (Budapest: Akademiai Kiado)
- Reed, C. B. 1996, *AJ*, 111, 804
- See, T. J. J. 1897, *AJ*, 17, 119
- Sher, D. 1962, *Obs.*, 82, 63
- Sher, D. 1965, *QJRAS*, 6, 299
- Shobbrook, R. R., & Lynga, G. 1994, *MNRAS*, 269, 857
- Trumpler, R. J. 1930, *Lick Obs. Bul.*, 14, 154
- Strömgren, B. 1966, *ARA&A*, 4, 433
- Vázquez, R. A., May, J., Carraro, G., et al. 2008, *ApJ*, 672, 930